Talanta 132 (2015) 294–300

Contents lists available at ScienceDirect

Talanta

journal homepage: www.elsevier.com/locate/talanta

Characterisation of biosynthesised silver nanoparticles by scanning electrochemical microscopy (SECM) and voltammetry

Dario Battistel [a,*], Franco Baldi [b], Michele Gallo [b], Claudia Faleri [c], Salvatore Daniele [b,**]

[a] Dipartimento di Scienze Ambientali, Infomatica e Statistica, University Cà Foscari Venice. Calle Larga Santa Marta 2137. 30127 Venice, (I)
[b] Dipartimento di Scienze Molecolari e Nanosistemi, University Cà Foscari Venice. Calle Larga Santa Marta 2137. 30127 Venice, (I)
[c] Dipartimento Scienze della Vita, Siena University, via Mattioli 4, 53100 Siena (I)

ARTICLE INFO

Article history:
Received 17 July 2014
Received in revised form
5 September 2014
Accepted 11 September 2014
Available online 19 September 2014

Keywords:
Silver nanoparticles
Bacteria
Biosynthesis
Scanning electrochemical microscopy
Anodic stripping voltammetry

ABSTRACT

Silver nanoparticles (AgNPs) were biosynthesised by a *Klebsiella oxytoca* strain BAS-10, which, during its growth, is known to produce a branched exopolysaccharide (EPS). *Klebsiella oxytoca* cultures, treated with $AgNO_3$ and grown under either aerobic or anaerobic conditions, produced silver nanoparticles embedded in EPS (AgNPs-EPS) containing different amounts of Ag(0) and Ag(I) forms. The average size of the AgNPs-EPS was determined by transmission electron microscopy, while the relative abundance of Ag (0)- or Ag(I)-containing AgNPs-EPS was established by scanning electrochemical microscopy (SECM). Moreover, the release of silver(I) species from the various types of AgNPs-EPS was investigated by combining SECM with anodic stripping voltammetry. These measurements allowed obtaining information on the kinetic of silver ions release from AgNPs-EPS and their concentration profiles at the substrate/water interface.

© 2014 Elsevier B.V. All rights reserved.

1. Introduction

Recently, a number of novel materials containing silver nanoparticles (AgNPs) have been introduced [1–3]. Their usage in commercial goods, such as cosmetics, apparels, medical and electrical devices [4,5], prompted researchers to investigate on AgNPs toxicity towards human cells, aquatic organisms [6] and, more in general, bacterial strains [7–10]. On the other hand, because of the latter property, AgNPs have received increasing attention as antimicrobial agents towards many Gram-positive and Gram-negative bacteria, fungi and viruses [11].

Nowadays, various methodologies are available for the synthesis of AgNPs [7,12–15], and are based on either chemical or biological approaches. The latter have received increasing attention due to the growing need of developing environmental-friendly technologies in material synthesis [12–14]. To this purpose, several microorganisms have been explored as potential cell-factories for both intra- and extracellular synthesis of nanoparticles of various metals [14]. For the biological synthesis of AgNPs, a variety of microorganisms, coming from bacteria and fungi, have been reported [16–19]. The mechanism is related to multiple phenotypic characteristics of the microorganisms, which can produce polymers, such as polysaccharides [20], which can, consequently, embed and stabilise the metal nanoparticles. These AgNPs-containing materials, in view of their biocompatibility, have potential applications as antimicrobials, especially in biomedical fields and food packaging [6,10,20].

The toxicity of AgNPs depends on several properties of the nanoparticles such as size and shape, surface area and charge, capping agents, bioavailability of the individual particles or silver forms [21–23]. With regard to the latter aspect, it is not yet clear whether the AgNPs toxic effects are due to the release of free Ag^+, the nanoparticles themselves or a combination of both species [24–27]. Therefore, investigations on the AgNPs redox properties and their reactivity at interfaces with aqueous environments is highly desirable.

Scanning electrochemical microscopy (SECM) is gaining increasing applications for the in situ investigation of localised phenomena and reactivity of substrates with high spatial resolution [28]. SECM is a scanning probe microscopy technique, which is based on the amperometric signal generated at a microelectrode by redox-active species in solution, which can perform quantitative local electrochemical experiments for studying heterogeneous and homogeneous reactions [29], for high-resolution imaging of the chemical reactivity and topography of various interfaces and surfaces [30,31]. In the field in which the present work falls, SECM has been used to characterise antimicrobial silver films [32], to

* Corresponding author. Tel.: +39 041 234 8506.
** Corresponding author.
E-mail addresses: dario.battistel@unive.it (D. Battistel), sig@unive.it (S. Daniele).

http://dx.doi.org/10.1016/j.talanta.2014.09.023
0039-9140/© 2014 Elsevier B.V. All rights reserved.

evaluate the interaction between Ag(I) ions and fibroblast cells [33] and to establish the effect of AgNPs on HeLa cells activity [34]. Aspects concerning the characterisation of pristine biosynthesised AgNPs in terms of oxidation state of silver and release of silver ions at interfaces have been less investigated. In fact, AgNPs could contain Ag(0), Ag(I) or both forms, this implying a different reactivity upon their contact with water [35].

Recently, it has been reported that *Klebsiella oxytoca (KO)* cultures, treated with $AgNO_3$ solutions, are able to synthesise AgNPs [36], which are embedded in branched exopolysaccharides (EPS) (AgNPs-EPS) [37]. These materials, produced under aerobic ($AgNPs^{aer}$-EPS) or anaerobic ($AgNPs^{anaer}$-EPS) conditions, could contain various forms of silver species and therefore could manifest different reactivity.

In this article, we report an SECM-voltammetric investigation devoted at establishing the oxidation state and reactivity of AgNPs-EPS biosynthesised by a strain of *KO*, and evaluating the amount of diffusable Ag(I) released at the substrate/solution interface.

2. Materials and methods

2.1. Materials and microbial strain

All chemicals were of reagent-grade and used as received, unless otherwise stated. Potassium hexachloroiridate(III) (Sigma Aldrich) was used as redox mediator in SECM investigations. The Nutrient Broth was purchased from Difco. Glycerol, sodium hydrogen carbonate, ammonium nitrate, magnesium sulphate heptahydrate, sodium dihydrogen phosphate, potassium acetate, sodium citrate, sodium hydroxide and silver nitrate were purchased from Sigma Aldrich. The chloride-free NAC medium, used for cell cultures, contained: 2.5 g l^{-1} sodium hydrogen carbonate, 1.2 g l^{-1} ammonium nitrate, 1.5 g l^{-1} magnesium sulphate heptahydrate, 0.6 g l^{-1} sodium dihydrogen phosphate, 0.132 g l^{-1} potassium acetate and 14.7 g l^{-1}sodium citrate. *Klebsiella oxytoca* was isolated from acid mine drainage of pyrite mines as reported in detail elsewhere [38].

2.2. Cultivation of K. oxytoca BAS-10 and production of AgNPs-EPS

Aerobic and anaerobic AgNPs-EPS were prepared as follows. 200 μL of a suspension containing *KO* BAS-10 cells, kept in cryovials at −80 °C in 25% glycerol and Nutrient Broth, were finally inoculated in chloride-free NAC medium. The pH of the NAC medium was previously adjusted to pH 7.6, by adding NaOH [39]. The *KO* BAS-10 cultures were grown both in aerobic and anaerobic conditions, at a controlled temperature of 30 °C. Aerobic conditions were ensured by stirring the cultures with an orbital stirrer under air-exposed media. For the anaerobic growth, the cultures were placed in a pirex bottle that had been previously saturated with nitrogen, then sealed and maintained under nitrogen blanket. At stationary phase of growth, $AgNO_3$ (to provide 50 mg L^{-1} of total Ag) was added to both types of *KO* BAS-10 cultures. These were left for 24–48 hours, till the metal-enriched polysaccharide flocculated in the bottom of the flask. AgNPs-EPS obtained in both aerobic and anaerobic conditions were subsequently separated by centrifugation and then treated with cooled ethanol in order to obtain a final hydroalcoholic solution 70% v/v. The colloidal materials were kept at 5 °C overnight, dried out under vacuum and grinded in a mortar.

2.3. TEM measurements on AgNPs-EPS

For the analysis of TEM, 1 mg each of $AgNPs^{aer}$-EPS and $AgNPs^{anaer}$-EPS was suspended in 1 ml of milli-Q water and sonicated for 10 min. Then, a 5 μl aliquot of each suspension was placed on a platinum grid coated with Formovar resin and then allowed to dry prior to TEM observations. The TEM images of the AgNPs were obtained using a JEOL JEM 100b (Tokyo, Japan) operating under standard conditions. The size distribution of the AgNPs was determined by image analyses of micrographs using the free source software Image J64 (NIH, USA).

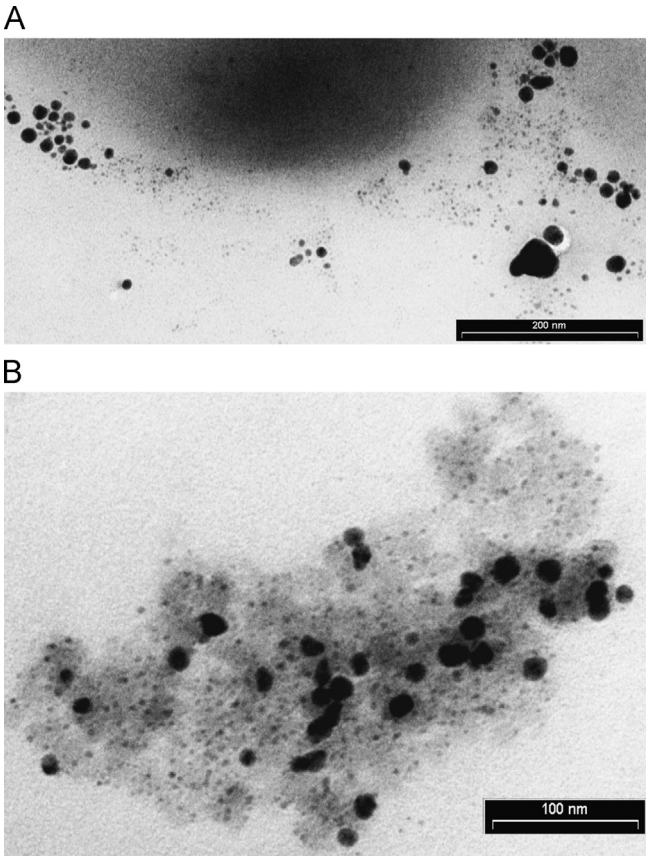


Fig. 1. TEM micrographs obtained on AgNPs-EPS obtained in anaerobic **(A)** and aerobic conditions **(B)**.

2.4. SECM and voltammetric experiments on AgNPs-EPS

SECM and voltammetric experiments were performed in a two-electrode cell, which comprised a working (or SECM tip) electrode and a reference/counter electrode. Platinum disk microelectrodes with nominal radius of 12.5 μm were employed as tip/working electrodes in either SECM or voltammetric measurements. They were prepared by sealing platinum wires within glass capillaries [40]. Afterward, they were tapered to a conical shape, polished with graded alumina powder (5, 1 down to 0.3 μm) and then characterised by cyclic voltammetry at low scan rates and by SECM to evaluate the actual electrode radius of the microelectrode and the overall tip radius to the electrode radius ratio (*RG*) [28,40]. The tips employed here had *RG* values over the range of 8–10. In all electrochemical measurements, a reference/counter electrode Ag/AgCl in saturated KCl was used. A CHI920B workstation (CH Instruments) was employed for both SECM and voltammetric experiments. Measurements, for establishing the oxidation state of the various types of AgNPs (immobilised onto a glass substrate as described below) by SECM, were performed in solutions containing 1 mM K_3IrCl_6 as redox mediator, and 0.1 M KNO_3 as supporting electrolyte. Diffusion controlled oxidation of $IrCl_6^{3-}$ at the SECM tip (vide infra) was achieved by applying a constant potential (E_{tip}) of +0.9 V (see inset in Fig. 2). Current against tip to substrate distance plots (i.e., approach curves) were constructed using normalised currents, $I_N = I/I_{bulk}$, (I is the actual tip current; I_{bulk} is the current

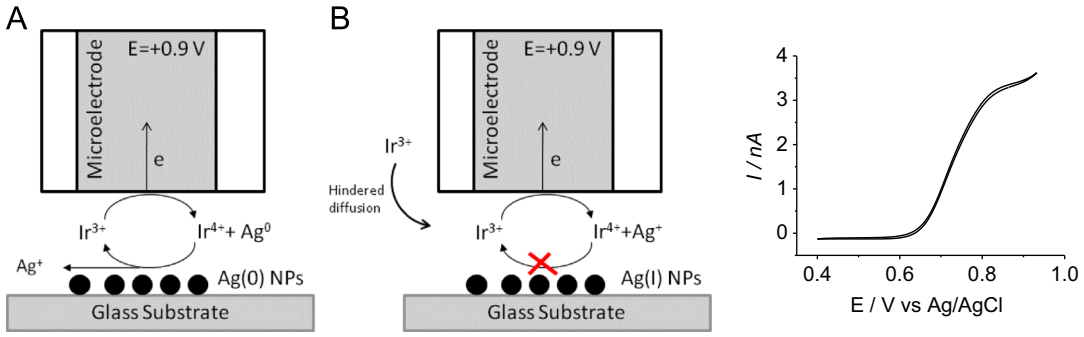


Fig. 2. Schematics of the operating principle for SECM measurements involving: **(A)** negative feedback on Ag(I)NPs and **(B)** positive feedback on Ag(0)NPs. Inset: cyclic voltammetry recorded with a Pt microdisc 12.5 μm radius in a 1 mM K_3IrCl_6+0.1 M KNO_3 solution. Scan rate 10 mV s^{-1}.

measured in the bulk of the solution), against normalised distances $L=d/a$ (d is the tip-substrate distance and a is the microdisc radius). Normalised currents were also used for drawing SECM line scans. For voltammetric and SECM measurements of Ag(I) species, the electrolyte solution consisted of 0.1 M KNO_3. In this measurements, the tip-substrate distance was determined by using the negative feedback approach curves recorded employing oxygen, dissolved in the aerated solution, as redox mediator [41]. The release of silver ions was monitored by using anodic stripping voltammetry (ASV) [42]. Unless otherwise stated, all electrochemical measurements were performed in aerated solutions.

2.5. Immobilisation of the AgNPs-EPS for SECM and voltammetric experiments

For both SECM and voltammetric measurements, $AgNPs^{aer}$-EPS and $AgNPs^{anaer}$-EPS were immobilised onto glass slides. The latter were first washed with ethanol, rinsed with distilled water and dried with nitrogen. The clean slides were afterward soaked in 10% poly-L-lysine (Sigma Aldrich) solutions for 5 min and then dried under chemical hood at 60 °C for 1 h. 20 μL of aqueous suspensions containing 10 mg ml^{-1} AgNPs-EPS were placed on the poly-L-lysine layer [33] and dried at 30 °C overnight. This procedure allowed obtaining several series of three spots (each about 3 mm diameter) of each type of AgNPs-EPS samples.

3. Results and discussion

3.1. TEM analysis

Fig. 1 shows typical TEM micrographs of the $AgNPs^{aer}$-EPS (Fig. 1 A) and $AgNPs^{anaer}$-EPS (Fig. 1B) samples investigated. The high electron-dense spots, due to AgNPs, are embedded on the polysaccharide matrix, and display, predominantly, a spherical shape. Digital analysis provided an average size of 11 ± 5 nm. This value is within those obtained for AgNPs produced by using other bacterial exopolysaccharides [20].

3.2. SECM investigation

The oxidation state of the silver species present in the AgNPs-EPS was investigated by using SECM, operating in the feedback mode in a solution containing K_3IrCl_6 as redox mediator. With this procedure, two phenomena could be observed depending on whether the sample examined was unreactive (or insulating) or reactive (or conducting) [28]. In the first case, the current decreased as the microelectrode, from the bulk solution, was brought towards the substrate (negative feedback); in the second case, the current increased due to the recycling of the redox mediator at the SECM tip (positive feedback). Under our conditions, negative or positive feedback occurred depending on whether the AgNPs-EPS substrates contained Ag(I)NPs or Ag(0) NPs, respectively. This can be understood by considering the scheme shown in Fig. 2. When the substrate contains Ag(0)NPs (Fig. 2 A), the following electrochemical reactions can occur:

$$IrCl_6^{3-} \rightarrow IrCl_6^{2-} + e- \quad (1)$$

reaction at the tip

$$IrCl_6^{2-} + Ag(0) \rightarrow IrCl_6^{3-} + Ag^+ \quad (2)$$

reaction at the substrate

Reaction (2) represents a heterogeneous bimolecular electron transfer process, which is shifted towards the right hand side because the standard redox potential of the $IrCl_6^{2-}/IrCl_6^{3-}$ couple is higher than that of the Ag(I)/Ag(0) species. Thus, when the tip is close to the substrate, the redox mediator is regenerated and the current increases. On the other hand, in the presence of Ag (I) species, reaction (2) does not occur and the substrate hinders the diffusion of the redox mediator (Fig. 2B) [28]. Fig. 3A shows typical normalised current against normalised distance plots recorded while approaching the microelectrode to the $AgNPs^{aer}$-EPS or $AgNPs^{anaer}$-EPS spots. For comparison, approach curves recorded above a clean glass surface, at an EPS sample produced by *KO* cells untreated with $AgNO_3$, and theoretical diffusion controlled approach curves for either positive (red straight line) or negative feedback (blue dashed line) are shown. It is evident that above both the $AgNPs\text{-}EPS^{aer}$ and $AgNPs\text{-}EPS^{anaer}$ spots, positive feedback is recorded. On the other hand, above either the clean glass surfaces or the Ag-free EPS, negative feedback responses are obtained. These results indicate that in both types of materials reaction mechanism (1)–(2) is operative, thus denoting the presence of Ag(0) species. However, the extent of positive feedback, at a given tip to substrate distance, depends on the specific sample investigated, it being larger above the $AgNPs^{anaer}$-EPS. This is conceivably due to a higher amount and readily available Ag(0)NPs in the latter sample with respect to the $AgNPs^{aer}$-EPS. Instead, as expected, negative feedback responses were recorded above either the clean glass surface or the AgNPs-free EPS samples, where reaction (1)–(2) cannot occur. It must be considered that negative approach curves (as those for the glass slide) were also recorded in some zones of the AgNPs-EPS spots investigated, indicating that, locally, either AgNPs-EPS rich of Ag(I) NPs or no AgNPs-EPS material was present.

The distribution and density of Ag(0) in the AgNPs-EPS materials was evaluated by SECM operating in line-scanning mode. These experiments were performed by positioning the SECM tip at ~10 μm above the sample and then recording the current along

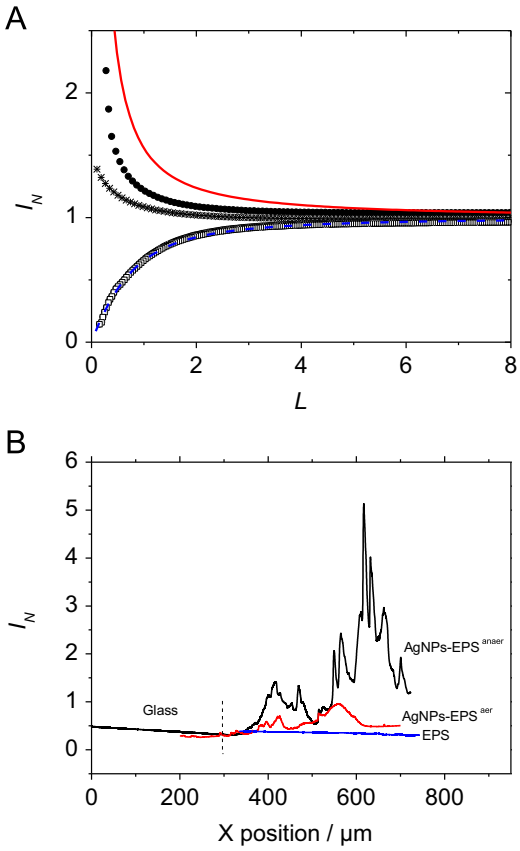


Fig. 3. **(A)** Approach curves recorded above: (∗) AgNPs^{aer}-EPS; (•) AgNPs^{aenaer}-EPS; (⋄) a clean glass surface; (○) EPS untreated with $AgNO_3$; theoretical for (red line) positive and (black line) negative feedback approach curves. **(B)** SECM line-scans recorded above a border region between the clean glass slide and (black line) Ag-NPs^{anaer}-EPS, (red line) Ag-NPs^{aer}-EPS; (blue line) Ag-free EPS.

the x (or y) direction. Fig. 3B shows typical SECM line scans recorded above a border region between the clean glass slide and the AgNPs^{anaer}-EPS (black line) or AgNPs^{aer}-EPS (red line) spots. As is evident, current increments, conceivably due to the positive feedback effect, were recorded when the microelectrode travelled above both types of spots (from 350 to 700 μm in Fig. 3B). Instead, low and almost constant currents were recorded as long as the microelectrode was moved above the glass slides (from 0 to 350 μm in Fig. 3B). Line scans with similar features and low current changes were also obtained above the AgNPs-free EPS samples (see blue line in Fig. 3B). In this case, the current change was essentially due to the roughness of the samples investigated, which could also affect the tip current responses [44]. The latter finding also indicates that the topography of the investigated samples is flat enough and does not affect significantly the overall current responses due to the AgNPs-EPS film.

Comparing the line scans recorded above the AgNPs-EPS samples, it is evident that normalised currents were, in general, higher above the AgNPs^{anaer}-EPS spot, confirming that the latter sample contained larger amounts of Ag(0)NPs as previously observed comparing the positive feedback approach curves. Form TEM images and considering that the EPS matrix provided images of quite flat surfaces, at this level of resolution, it is reasonable to assume that the roughness of the AgNPs-EPS samples does not affect the feedback current responses.

Considering again Fig. 3A, it is evident that the approach curves, recorded above both types of AgNPs-EPS spots, in no case fit that for diffusion controlled positive feedback. This could be attributed to several factors, including the facts that the Ag(0)NPs, embedded in the polysaccharide matrix, do not form large interconnected silver clusters, or that the kinetic of the heterogeneous bimolecular electron transfer process, involved in reaction (2), is not fast. At this stage, we are unable to differentiate among the various factors.

3.3. Study of the release of Ag(I) species

Information on reactivity of AgNPs and the release of Ag(I) species at the AgNPs-EPS/water interface was obtained by combining SECM and voltammetric experiments. The measurements were performed on AgNPs-EPS modified glass-slide spots immersed in a 0.1 M KNO_3 aerated-aqueous solution. Under these conditions, Ag(I) species, eventually present in the samples, or formed by corrosion of Ag(0)NPs, could diffuse to the aqueous solution and thereby collected at the microelectrode tip (scheme in Fig. 4). In these experiments, the tip-substrate distances were established using oxygen (from the air saturated solution) as redox mediator. Oxygen was used in order to avoid any possible interference due to the oxidising action of the $IrCl_6^{2-}/IrCl_6^{3-}$ couple towards Ag(0)NPs.

Evidences for the formation of Ag(I) species or the presence of soluble Ag(0)NPs were, initially, gained by using cyclic voltammetry (CV) with the microelectrode positioned at 10 μm above the substrates. Cyclic voltammograms were recorded in the potential window from 0.05 to 0.80 V, where both reduction of Ag(I) species and oxidation of Ag(0), accumulated at the microelectrode surface, could occur [43]. Fig. 5 shows a typical CV recorded at 50 mV s^{-1} with the Pt microdisc positioned above a AgNPs^{aer}-EPS spot, after 2 hours the introduction of the 0.1 M KNO_3 solution. The potential was initially scanned from the rest potential (0.25 V) towards

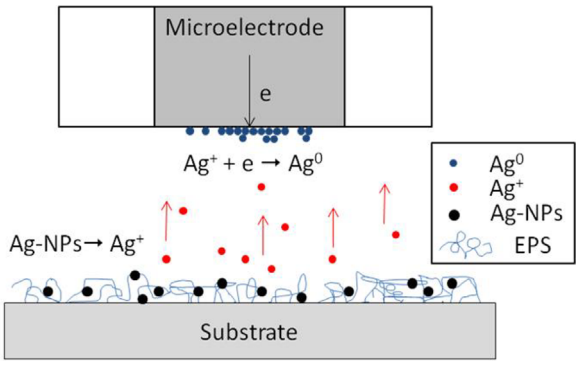


Fig. 4. Schematic of the Ag(I) species release from the AgNPs-EPS substrate and collection at the SECM tip.

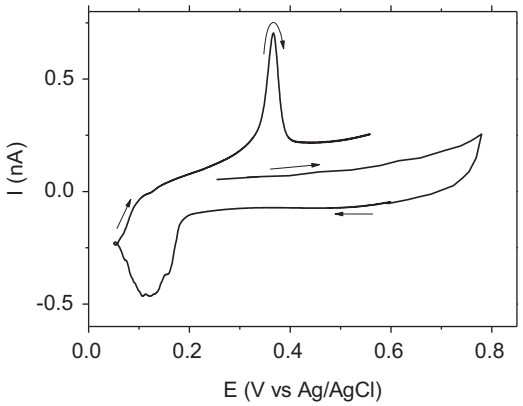


Fig. 5. Cyclic voltammograms recorded by using a 12.5 μm Pt microelectrode placed 10 μm above a Ag-EPS^{aer} spot after two hours immersion in a 0.1 M KNO_3 aqueous solution. Scan rate: 50 mV s^{-1}

positive potentials, to oxidise, eventually, soluble or colloidal Ag(0) NPs-containing compounds; then from the anodic limit the potential was scanned towards negative potentials where Ag (I) species could be reduced; afterwards, the potential was scanned again towards positive values to oxidise Ag(0) accumulated at the electrode surface. As is evident from Fig. 5, no wave is observed during in first anodic scan, indicating that no or negligible amount of Ag (0) was present within the microelectrode/substrate gap. Instead, a cathodic peak at 0.2 V and an anodic one at 0.4 V, due to the reduction of the Ag(I) species and the oxidation of Ag(0) accumulated onto the electrode surface, respectively, were obtained during the subsequent negative and positive scans. The peak shaped response, obtained in the cathodic scan, instead of a steady-state (or pseudo-steady state, typical for microelectrodes) [45], suggested a thin layer behaviour [46] and that almost all Ag(I) species, present within the tip/substrate gap, were depleted.

CVs similar to that shown in Fig. 5 were also obtained above a AgNPs^{anaer}-EPS sample (not shown). However, in the latter case, valuable voltammograms could be obtained only after longer (i.e. 4–5 h) immersion times of the sample in the water solution. This finding suggested that the Ag(I) species released from AgNPs^{anaer}-EPS, which is richer of Ag(0)NPs, involved a more complex pathway, including the metal corrosion process.

To achieve a better sensitivity in the measurements, and for quantitative determination of silver(I) species released from the AgNPs-EPS samples, anodic stripping voltammetry was employed [47,48]. A first series of ASVs was carried out for obtaining information on the dissolution rate of the Ag(I) species. To this purpose, the Pt microelectrode was positioned at 10 μm above the samples and ASVs were recorded with time. The ASVs were performed using a deposition time of 60 seconds, a deposition potential equal to −0.1 V vs. Ag/AgCl and linear sweep voltammetry at 50 mV s^{-1} during the stripping step. Fig. 6A B show typical ASVs thus recorded for different elapsed times after the samples had been immersed in the water solution. For both samples, the stripping peak height increases with time, confirming that increasing amounts of Ag(I) species dissolved to the water phase. The concentration (C^b_{Ag+}) was estimated by comparing the anodic charge involved in the ASV peaks, recorded above the AgNPs-EPS samples, to those obtained in $AgNO_3$ solutions of known concentrations. Fig. 6C shows plot of C^b_{Ag+} against immersion time (t_i). It is evident that the Ag(I) concentration increases with time for both AgNPs-EPS samples; however, after about 20 and 25 min for the AgNPs-EPS^{aer} and AgNPs-EPS^{anaer} sample, respectively, the concentration levels off. This is probably due to the achievement of an equilibrium between soluble Ag(I) and Ag(I)

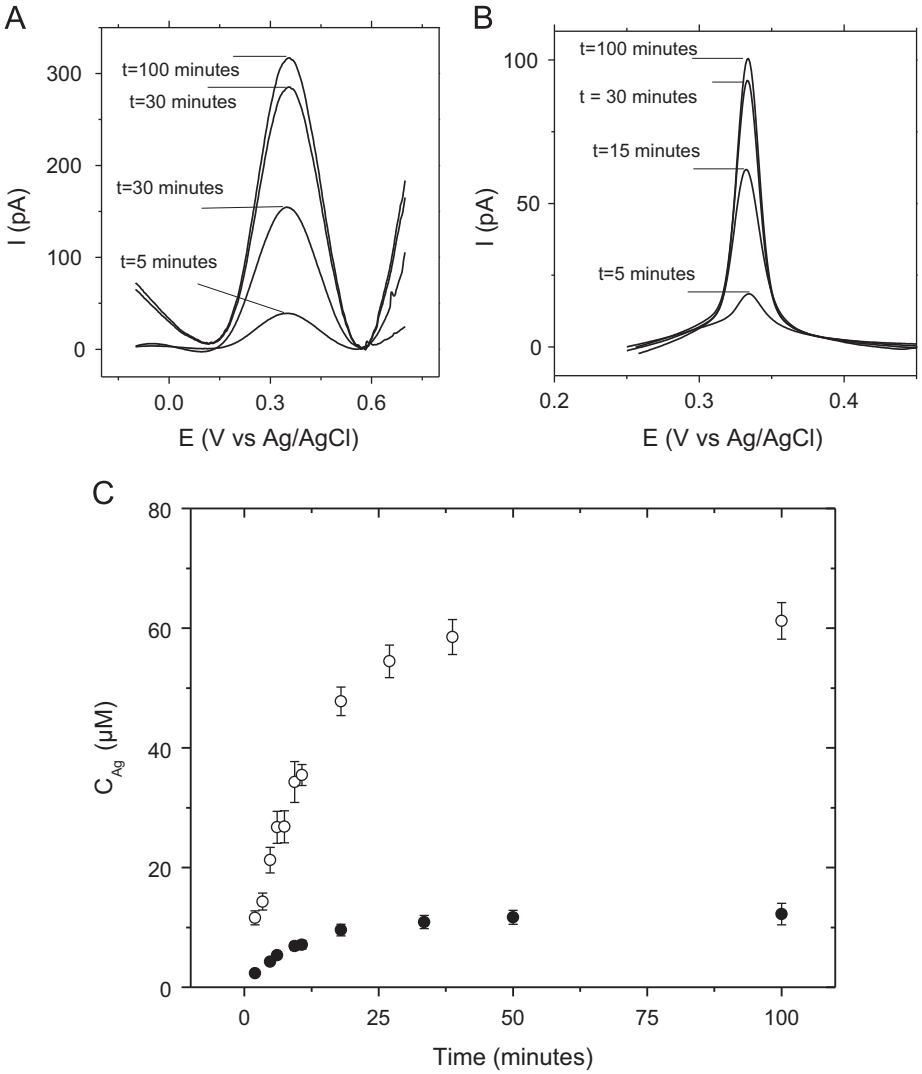


Fig. 6. ASVs recorded at different times with a Pt microdisc positioned at 10 μm above **(A)** Ag^{aer}NPs-EPS and **(B)** Ag^{anaer}NPs-EPS. **(C)** Concentration against elapsed time after immersion in the 0.1 M KNO_3 solution of (○) Ag-NPs^{aer}-EPS and (●)Ag-NPs^{anaer}-EPS samples. ASVs parameters: deposition time 60 s, deposition potential −0.1 V and, 50 mV s^{-1}during the stripping step. Error bars are established on the basis of three consecutive ASVs.

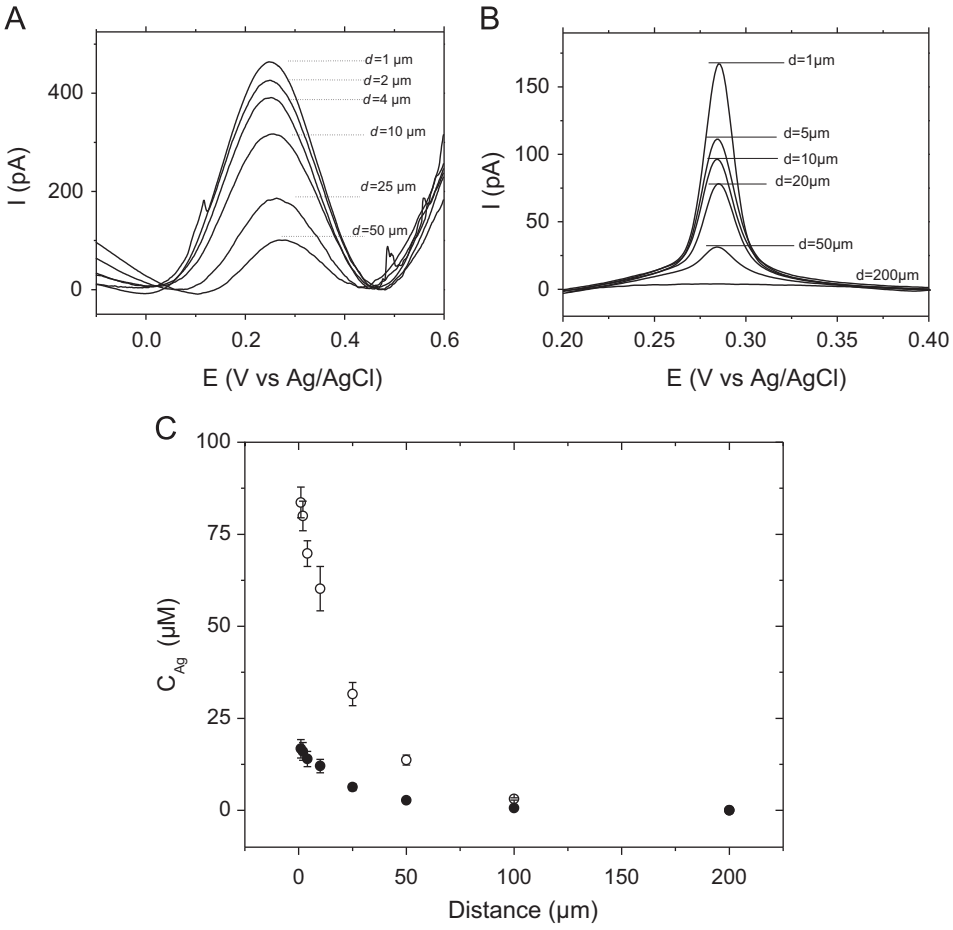


Fig. 7. ASVs recorded at different tip-substrate distances with a Pt microdisc after the samples had been immersed in 0.1 M KNO_3 for 30 minutes. **(A)** for $AgNPs^{aer}$-EPS and **(B)** $AgNPs^{anaer}$-EPS. **(C)** Concentration profiles for (○) $AgNPs^{aer}$-EPS and (●) $Ag\text{-}NPs^{anaer}$-EPS. ASVs parameters: deposition time 60 s, deposition potential -0.1 V and scan rate, during the stripping step, 50 mV s^{-1}. Error bars are calculated on the basis of three consecutive ASVs.

NPs-EPS bound species. It is interesting to note that the amount of Ag(I) released from $AgNPs^{aer}$-EPS is sensibly higher (4–6 times) than that of $AgNPs^{anaer}$-EPS. These results therefore, once again, confirm that the composition of the AgNPs-EPS materials are differently rich of Ag(I)NPs or Ag(0)NPs.

The concentration profiles of Ag(I) species at the samples samples/solution interface at equilibrium (i.e., at the time where C^b achieved the plateau region, in the present case 30 min) were also evaluated by performing a further series of measurements in which ASVs were recorded at different tip to substrate distances (Fig. 7A,B). Fig. 7C shows concentration against distance plots, and, as is evident, for both samples the amount of Ag(I) species in the solution decreases as the tip-substrate distance increases. For distances greater than 100 μm, the amount of Ag(I) was not detectable under the above ASV conditions. These results, again, support the circumstance that multiple equilibria involving Ag(I)-bound to AgNPs-EPS or sparingly soluble species affect the overall dissolution process. Also in these measurements, the amount of Ag(I) released from $AgNPs^{aer}$-EPS is higher than that of $AgNPs^{anaer}$-EPS.

4. Conclusion

In this work, AgNPs, embedded in an exopolysaccharide matrix, biosynthesised using a *K. oxytoca* BAS-10 strain, have been characterised to establish their chemical properties and reactivity at the sample/solution interface. This information has been gathered by using scanning electrochemical microscopy and voltammetry. This study has proven that Ag(0) or Ag(I) forms are present in the AgNPs-EPS materials and their abundance depends on whether the materials were prepared under aerobic or anaerobic conditions. As expected, Ag(I) forms predominate in the $AgNPs^{aer}$-EPS material, conceivable due to the presence of oxygen, which could promote the oxidation of Ag(0)NPs to provide easier diffusable Ag(I) species. This could imply a potentially higher antimicrobial activity of the $AgNPs^{aer}$-EPS composite. The antibacterial activity of both $AgNPs^{aer}$-EPS and $AgNPs^{aner}$-EPS towards both Gram-positive and Gram-negative bacteria is currently under investigation in our laboratory.

Acknowledgement

Financial support of the Ministry of University and Scientific Research (MIUR) (PRIN-2010AXENJ8) is gratefully acknowledged.

References

[1] S. Siripattanakul-Ratpukdi, M. Fürhacker, Water Air Soil Poll 225 (2014) 1–18.
[2] N. Vigneshwaran, A.A. Kathe, P.V. Varadarajan, R.P. Nachane, R.H. Balasubramanya, J. Nanosci. Nanotechnol. 7 (2007) 1893–1897.
[3] A. Goyal, A. Kumar, P.K. Patra, S. Mahendra, S. Tabatabaei, P.J.J. Alvarez, G. John, P.M. Ajayan, Macromol. Rapid Commun. 30 (2009) 1116–1122.
[4] N. Singh, B. Manshian, G.J. Jenkins, S.M. Griffiths, P.M. Williams, T.G. Maffeis, C.J. Wright, S.H. Doak, Biomaterials 30 (2009) 3891–3914.
[5] G. Oberdorster, E. Oberdorster, J. Oberdorster, Environ. Health Persp. 113 (2005) 823–839.
[6] A.K. Suresh, D.A. Pelletier, M.J. Doktycz, Nanoscale 5 (2013) 463–474.

[7] A. Hebeish, M.E. El-Naggar, M.G.M. Fouda, M.A. Ramadan, S.S. Al-Deyab, S. Salem S., M.H. El-Rafie, Carbohydr. Polym 86 (2011) 936–940.
[8] V.K. Sharma, R.A. Yngard, Y. Lin, Adv. Coll. Interf. Sci. 145 (2009) 83–96.
[9] J.R. Morones, J.L. Elechiguerra, A. Camacho, K.B. Holt, J.B. Kouri, J.T. Ramirez, M.J. Yacaman, Nanotechnology 16 (2005) 2346–2353.
[10] A.M. Fayaz, K. Balaji, M. Girilal, P.T. Kalaichelvan, R. Venkatesan, J. Agric. Food Chem. 57 (2009) 6246–6252.
[11] M. Sureshkumar, D.Y. Siswanto, C.K. Lee, J. Mat. Chem 20 (2010) 6948–6955.
[12] N. Vigneshwaran, R.P. Nachane, R.H. Balasubramanya, P.V.A. Varadarajan, Carbohydr. Res. 341 (2006) 2012–2018.
[13] A. Panacek, L. Kvitek, R. Prucek, M. Kolar, R. Vecerova, N.J. Pizurova, J. Phys. Chem. B 110 (2006) 16248–16253.
[14] K.B. Narayanan, N. Sakthivel, Adv. Coll. Interf. Sci. 156 (2010) 1–13.
[15] D. Wei, W. Sun, W. Qian, Y. Ye, X. Ma, Carbohydr. Res. 344 (2009) 2375–2382.
[16] A.K. Gade, P. Bonde, A.P. Ingle, P.D. Marcato, N. Duran, M.K. Rai, J. Biobased Mater. Bioenerg. 3 (2008) 123–129.
[17] G. Li, D. He, Y. Qian, B. Guan, S. Gao, Y. Cui, Int. J. Mol. Sci. 13 (2012) 466–476.
[18] V. Deepak, K. Kalishwaralal, S.R.K. Pandian, S. Gurunathan, in Metal Nanoparticles in Microbiology, Berlin (2011).
[19] G. Yang, J. Xie, Y. Deng, Y. Bian, F. Hong, Carbohydr. Polym 87 (2012) 2482–2487.
[20] P. Kanmani, S.-T. Lim, Process Biochem. 48 (2013) 1099–1106.
[21] A. Yu, X. Jiang, Q. Zeng, Chapter 17: Silver Nanoplates: Synthesis, Growth and Functional Properties, in: A. Barrañón (Ed.), New Nanotechnology Developments, Nova Science Publishers, UK, 2009.
[22] B. Fubini, I. Fenoglio, M. Ghiazza, Nanotoxicology 4 (2010) 347–363.
[23] R. Tantra, J. Tompkins, P. Quincey, Coll. Surf. B Biointer. 75 (2010) 275–281.
[24] N. Lubick, Environ. Sci. Technol. 42 (2008) 8617 8617.
[25] H.J. Johnston, G. Hutchison, F.M. Christensen, S. Peters, S. Hankin, V. Stone, Crit. Rev. Toxicol. 40 (2010) 328–346.
[26] M. Ahamed, M.S. AlSalhi, M.K.J. Siddiqui, Clin. Chim. Acta. 411 (2010) 1841–1848.
[27] M. Hadioui, S. Leclerc, K.J. Wilkinson, Talanta 105 (2013) 15–19.
[28] A.J. Bard, M.V. Mirkin, Scanning Electrochemical Microscopy, Marcel Dekker, New York, 2001.
[29] C.G. Zoski (Ed.), Handbook of Electrochemistry, Elsevier, Amsterdam, 2007.
[30] S. Bergner, P. Vatsyayan, F.-M. Matysik, Anal. Chim. Acta 775 (2013) 1–13.
[31] K. Kranz, Analyst 139 (2014) 336–352.
[32] F.-R.F. Fan, A.J. Bard, J. Phys. Chem. B 106 (2002) 279–287.
[33] K.B. Holt, A.J. Bard, Biochemistry 44 (2005) 13214–13223.
[34] Z. Chen, S.B. Xie, L. Shen, Y. Du, S.L. He, Q. Li, Z.W. Liang, X. Meng, B. Li, X.D. Xu, Analyst 133 (2008) 1221–1228.
[35] G.A. Sotiriou, A. Meyer, J.T.N. Knijnrnburg, S. Panke, S.E. Pratsinis, Langmuir 28 (2012) 15929–15936.
[36] F. Baldi, D. Battistel, S. Daniele, M. Gallo, S. Paganelli, O. Piccolo, C. Faleri, G. Gallo, A.M. Puglia, *In preparation*.
[37] S. Leone, C. De Castro, M. Parrilli, F. Baldi, R. Lanzetta, Eur. J. Org. Chem. 31 (2007) 5183–5189.
[38] F. Baldi, A. Minacci, M. Pepi, A. Scozzafava, FEMS Microbiol. Ecol. 36 (2001) 169–174.
[39] F. Baldi, D. Marchetto, S. Paganelli, O. Piccolo, New Biotechnol 29 (2011) 74–78.
[40] D. Battistel, S. Daniele, R. Gerbasi, M.A. Baldo, Thin Solid Films 518 (2010) 3625–3631.
[41] R.M. Souto, Y. Gonzalez-Garcia, D. Battistel, S. Daniele, Corros. Sci 55 (2012) 401–406.
[42] S. Daniele, I. Ciani, M.A. Baldo, C. Bragato, Electroanalysis 19 (2007) 2067–2076.
[43] D. Battistel, G. Pecchielan, S. Daniele, Chem. Electrochem 1 (2014) 140–146.
[44] D. Battistel, S. Daniele, D. Fratter, Electochim. Acta 78 (2012) 557–562.
[45] M.I. Montenegro, M.A. Queirós, J.L. Daschbach Microelectrodes, Theory and Applications, Kluwer, 1991.
[46] A.J. Bard, L.R. Faulkner, Electrochemical Methods, ed., Wiley, New York, 2001.
[47] J.V. Macpherson, P.R. Unwin, J. Phys. Chem. 100 (1996) 19475–19483.
[48] M.E. Abdelsalam, G. Denuault, S. Daniele, Anal. Chim. Acta 452 (2002) 65–75.